

SkewDB: A comprehensive database of GC and 10 other skews for over 28,000 chromosomes and plasmids

Bert Hubert*

*corresponding author: Bert Hubert (bert@hubertnet.nl)

ABSTRACT

GC skew denotes the relative excess of G nucleotides over C nucleotides on the leading versus the lagging replication strand of eubacteria. While the effect is small, typically around 2.5%, it is robust and pervasive. GC skew and the analogous TA skew are a localized deviation from Chargaff's second parity rule, which states that G and C, and T and A occur with (mostly) equal frequency even within a strand.

Most bacteria also show the analogous TA skew. Different phyla show different kinds of skew and differing relations between TA and GC skew.

This article introduces an open access database (<https://skewdb.org>) of GC and 10 other skews for over 28,000 chromosomes and plasmids. Further details like codon bias, strand bias, strand lengths and taxonomic data are also included. The *SkewDB* database can be used to generate or verify hypotheses. Since the origins of both the second parity rule, as well as GC skew itself, are not yet satisfactorily explained, such a database may enhance our understanding of microbial DNA.

Background & Summary

The phenomenon of GC skew is tantalizing because it enables a simple numerical analysis that accurately predicts the loci of both the origin and terminus of replication in most bacteria and some archaea¹².

Bacterial DNA is typically replicated simultaneously on both strands, starting at the origin of replication³. Both replication forks travel in the 5' to 3' direction, but given that the replichores are on opposite strands, topologically they are traveling in opposite directions. This continues until the forks meet again at the terminus. This means that roughly one half of every strand is replicated in the opposite direction of the other half. The forward direction is called the leading strand. Many plasmids also replicate in this way⁴.

The excess of G over C on the leading strand is in itself only remarkable because of Chargaff's somewhat mysterious second parity rule⁵, which states that within a DNA strand, there are nearly equal numbers of G's and C's, and similarly, T's and A's. This rule does not directly follow from the first parity rule, which is a simple statement of base pairing rules.

Depending on who is asked, Chargaff's second parity rule is so trivial that it needs no explanation, or it requires complex mathematics and entropy considerations to explain its existence⁶.

The origins of GC skew are still being debated. The leading and lagging strands of circular bacterial chromosomes are replicated very differently; it is at least plausible that this leads to different mutational biases. In addition, there are selection biases that are theorized to be involved⁷. No single mechanism may be exclusively responsible.

This article does not attempt to explain or further mystify⁸ the second parity rule or GC skew, but it may be that the contents of the *SkewDB* can contribute to our further understanding.

The *SkewDB* also contains some hard to explain data on many chromosomes. These include highly asymmetric skew, but also very disparate strand lengths. Conversely, the *SkewDB* confirms earlier work on skews in the Firmicute phylum⁹, and also expands on these earlier findings.

GC skew has often been investigated by looking at windows of DNA of a certain size. It has been found that the choice of window size impacts the results of the analysis. The *SkewDB* is therefore based exclusively on cumulative skew¹⁰, which sidesteps window size issues. For example, the sequence GGGCCC has a cumulative GC skew of zero, and as we progress through the sequence, this skew takes on values 1, 2, 3, 2, 1, 0.

The result of such an analysis is shown in figure 1. The analysis software fits a linear model on the skews, where it also compensates for chromosome files sequenced in the non-canonical direction, or where the origin of replication is not at the start of the file.

36 Methods

37 The *SkewDB* analysis relies exclusively on the tens of thousands of FASTA and GFF3 files available through the NCBI
38 download service, which covers both GenBank and RefSeq. The database includes bacteria, archaea and their plasmids.

39 Furthermore, to ease analysis, the NCBI Taxonomy database is sourced and merged so output data can quickly be related to
40 (super)phyla or specific species.

41 No other data is used, which greatly simplifies processing. Data is read directly in the compressed format provided by
42 NCBI. All results are emitted as standard CSV files.

43 In the first step of the analysis, for each organism the FASTA sequence and the GFF3 annotation file are parsed. Every
44 chromosome in the FASTA file is traversed from beginning to end, while a running total is kept for cumulative GC and TA
45 skew. In addition, within protein coding genes, such totals are also kept separately for these skews on the first, second and third
46 codon position. Furthermore, separate totals are kept for regions which do not code for proteins.

47 In addition, to enable strand bias measurements, a cumulative count is maintained of nucleotides that are part of a positive
48 or negative sense gene. The counter is increased for positive sense nucleotides, decreased for negative sense nucleotides, and
49 left alone for non-genic regions. A separate counter is kept for non-genic nucleotides.

50 Finally, G and C nucleotides are counted, regardless of if they are part of a gene or not.

51 These running totals are emitted at 4096 nucleotide intervals, a resolution suitable for determining skews and shifts.

52 In addition, one line summaries are stored for each chromosome. These line includes the RefSeq identifier of the
53 chromosome, the full name mentioned in the FASTA file, plus counts of A, C, G and T nucleotides. Finally five levels of
54 taxonomic data are stored.

55 Chromosomes and plasmids of fewer than 100 thousand nucleotides are ignored, as these are too noisy to model faithfully.
56 Plasmids are clearly marked in the database, enabling researchers to focus on chromosomes if so desired.

57 Fitting

58 Once the genomes have been summarised at 4096-nucleotide resolution, the skews are fitted to a simple model.

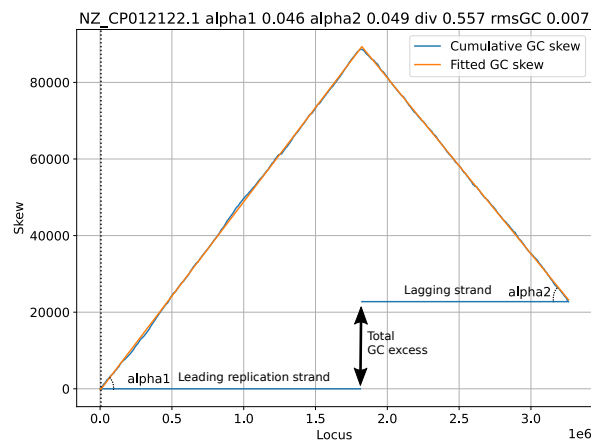


Figure 1. Sample graph showing *SkewDB* data for *Lactiplantibacillus plantarum* strain LZ95 chromosome

59 The fits are based on four parameters, as shown in figure 1. Alpha1 and alpha2 denote the relative excess of G over C
60 on the leading and lagging strands. If alpha1 is 0.046, this means that for every 1000 nucleotides on the leading strand, the
61 cumulative count of G excess increases by 46.

62 The third parameter is *div* and it describes how the chromosome is divided over leading and lagging strands. If this number
63 is 0.557, the leading replication strand is modeled to make up 55.7% of the chromosome.

64 The final parameter is *shift* (the dotted vertical line), and denotes the offset of the origin of replication compared to the
65 DNA FASTA file. This parameter has no biological meaning of itself, and is an artifact of the DNA assembly process.

66 The goodness-of-fit number consists of the root mean squared error of the fit, divided by the absolute mean skew. This latter
67 correction is made to not penalize good fits for bacteria showing significant skew.

68 GC skew tends to be defined very strongly, and it is therefore used to pick the *div* and *shift* parameters of the DNA
69 sequence, which are then kept as a fixed constraint for all the other skews, which might not be present as clearly.

70 The fitting process itself is a simplex (Amoeba) optimization over the three dimensions, seeded with the average observed
71 skew over the whole genome, and assuming there is no shift, and that the leading and lagging strands are evenly distributed.
72 The simplex optimization is tuned so that it takes sufficiently large steps so it can reach the optimum even if some initial
73 assumptions are off.

74 For every chromosome, plasmid and skew the model parameters are stored, plus the adjusted root mean squared error.

75 Both for quality assurance and ease of plotting, individual CSV files are generated for each chromosome, again at 4096
76 nucleotide resolution, but this time containing both the actual counts of skews as well as the fitted result.

77 **Some sample findings**

78 To popularize the database, an online viewer is available on <https://skewdb.org/view>.

79 **GC and TA skews**

80 Most bacteria show concordant GC and TA skew, with an excess of G correlating with an excess of T. This does not need
81 to be the case however. Figure 2 is a scatterplot that shows the correlation between the skews for various major superphyla.
82 Firmicutes (part of the Terrabacteria group) show clearly discordant skews.

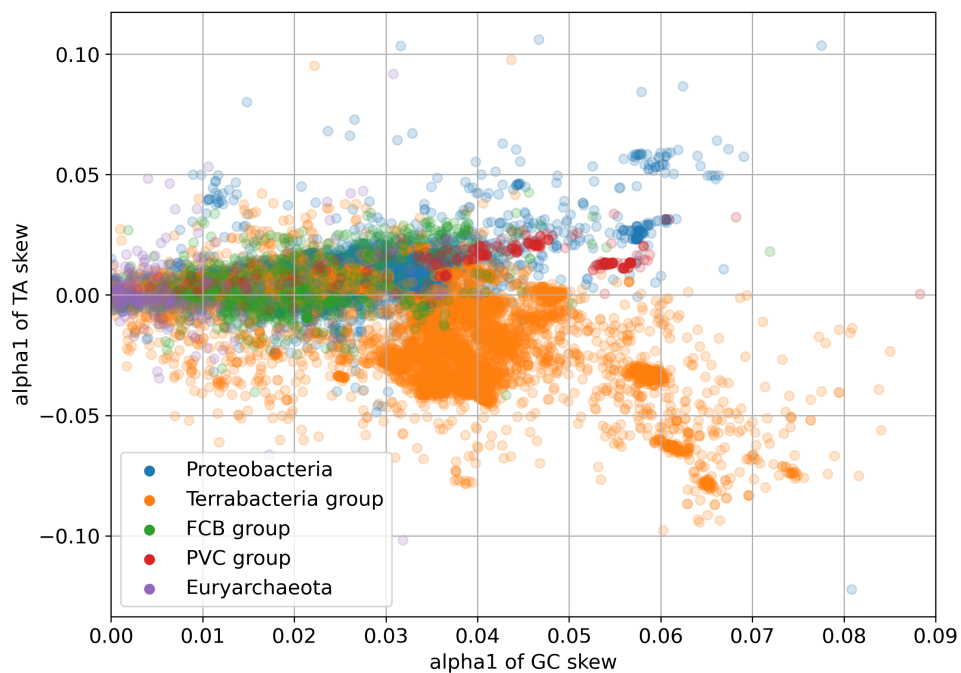


Figure 2. Scatter graph of 25,000 chromosomes by superphylum, GC skew versus TA skew

83 **Firmicute prediction**

84 In many bacteria, genes tend to concentrate on the leading replication strand. If the codon bias of genes is such that they are
85 relatively rich in one nucleotide, the “strand bias” may itself give rise to GC or TA bias. Or in other words, if genes contain a
86 lot of G’s and they huddle on the leading strand, that strand will show GC skew. As an hypothesis, we can plot the observed GC
87 and TA skews for all Firmicutes for which we have data.

88 Mathematically the relation between the codon bias, strand bias and predicted GC skew turns out to be a simple multiplication.
89 In figure 3, the x-axis represents this multiplication. The y-axis represents the GC and TA skew ratio.

90 It can clearly be seen that both GC and TA skew correlate strongly with the codon/strand bias product. TA skew goes to
91 zero with the two biases, but GC skew appears to persist even in the absence of such biases.

92 Figure 4 shows the situation within an individual chromosome (*C. difficile*), based on overlapping 40960-nucleotide
93 segments. On the x-axis we find the strand bias for these segments, running from entirely negative sense genes to entirely

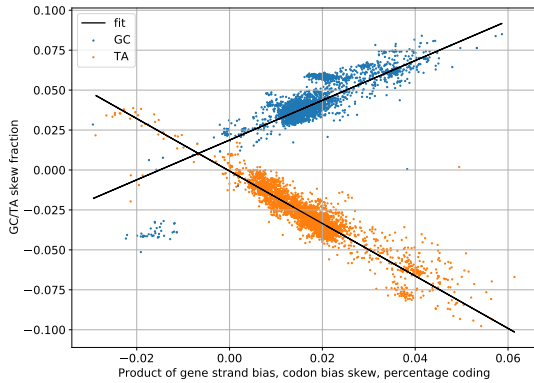


Figure 3. Predicted versus actual GC/TA skew for 4093 Firmicutes

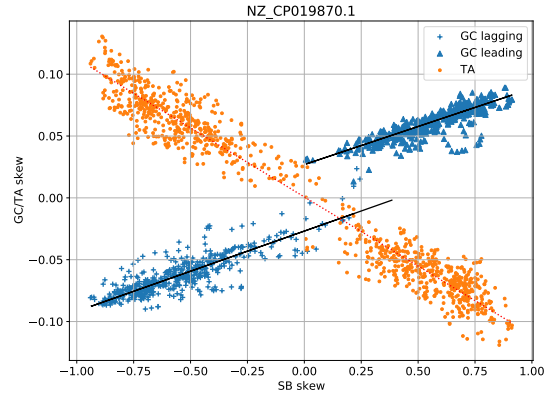


Figure 4. Scatter graph of codon/strand bias versus GC/TA skew for *C. difficile*

94 positive sense genes. The skew is meanwhile plotted on the y-axis, and here too we see that TA skew goes to zero in the absence
 95 of strand bias, while GC skew persists and clearly has an independent strand-based component.

96 **Asymmetric skew**

97 The vast majority of chromosomes show similar skews on the leading and the lagging replication strands, something that
 98 makes sense given the pairing rules. There are however many chromosomes that have very asymmetric skews, with one strand
 99 sometimes showing no skew at all. In figure 5 four chromosomes are shown that exhibit such behavior. The *SkewDB* lists
 100 around 250 chromosomes where one strand has a GC skew at least 3 times bigger/smaller than the other one.

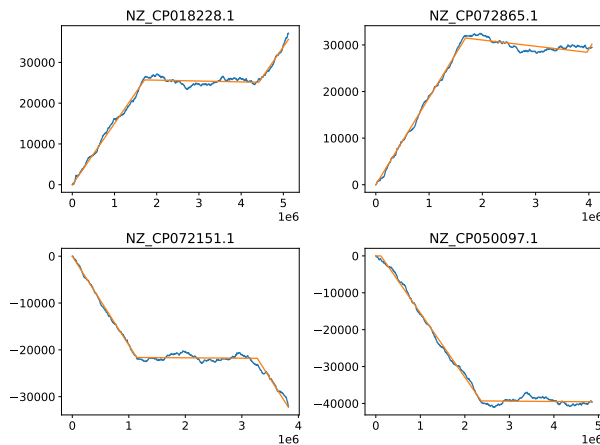


Figure 5. Chromosomes with asymmetric skews

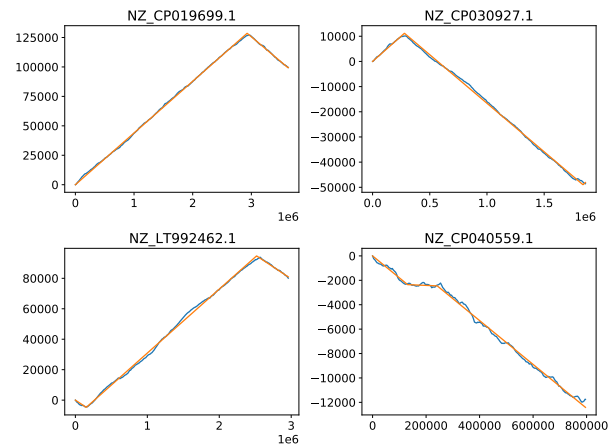


Figure 6. Chromosomes with differing strand lengths

101 **Asymmetric strands**

102 Bacteria tend to have very equally sized replication strands, which is also an optimum for the duration of replication. It is
 103 therefore interesting to observe that GC skew analysis finds many chromosomes where one strand is four times larger than the
 104 other strand. In figure 6 four such chromosomes are shown. The *SkewDB* lists around 100 chromosomes where one strand is at
 105 least three times as large as the other strand.

106 **Anomalies**

107 In many ways, GC skew is like a forensic record of the historical developments in a chromosome. Horizontal gene transfer,
 108 inversions, integration of plasmids, excisions can all leave traces. In addition, DNA sequencing or assembly artifacts will also
 109 reliably show up in GC graphs.

110 Figure 7 shows GC and TA skews for *Salmonella enterica subsp. enterica serovar Concord* strain AR-0407 (NZ_CP044177.1),
 111 and many things could be going on here. The peaks might correspond to multiple origins of replication, but might also indicate

112 inversions or DNA assembly problems.

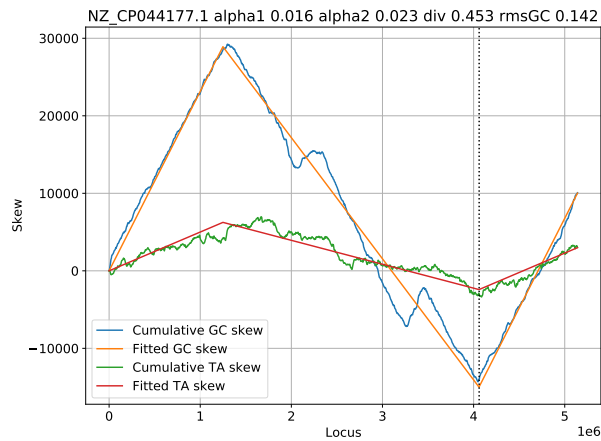


Figure 7. GC and TA skew for *Salmonella enterica* subsp. *enterica* serovar Concord strain AR-0407

113 Data Records

114 The *SkewDB* consists of several CSV files: *skplot.csv*, *results.csv*, *genomes.csv* and *codongc.csv*. In addition, for each
115 chromosome or plasmid, a separate *_fit.csv* file is generated, which contains data at 4096-nucleotide resolution.

116 *skplot.csv* contains all the 4096-nucleotide resolution data as one big file for all processed chromosomes and plasmids. The
parameters are described in table 1.

abspos	locus in chromosome	name	RefSeq ID
accounts0-4	A nucleotide counter	ngcount	Counter of non-coding nucleotides
ccounts0-4	C nucleotide counter	pospos	cumulative positive sense nucleotide counter
gcounts0-4	G nucleotide counter	relpos	relative position within chromosome/plasmid
tcunts0-4	T nucleotide counter	taskew	cumulative TA skew
gcskew	cumulative GC skew	taskew0-3	cumulative TA skew per codon position
gcskew0-3	cumulative GC skew per codon position	taskewNG	cumulative TA skew for non-coding regions
gcskewNG	cumulative GC skew for non-coding regions		

Table 1. Fields of *skplot.csv*

117

118 *results.csv* meanwhile contains the details of the fits. In this table 2, all marked out squares exist. The actual fields are
119 called *alpha1gc*, *alpha2gc*, *gcRMS*, *alpha1ta*, *alpha2ta* etc. DNA sequence shift and *div* are also specified, and they come from
120 the GC skew. *gc0-2*, *ta0-2* refers to codon position. *gcng* and *tang* refer to the non-coding region skews. Finally *sb* denotes the
121 strand bias.

	alpha1	alpha2	rms	div	shift
gc	X	X	X	X	X
ta	X	X	X		
gc0	X	X	X		
gc1	X	X	X		
gc2	X	X	X		
ta0	X	X	X		
ta1	X	X	X		
ta2	X	X	X		
gcng	X	X	X		
tang	X	X	X		
sb	X	X	X		

Table 2. Skew metrics

122 Table 3 documents the data on codon bias, also split out by leading or lagging strand found in codongc.csv.

afrac, cfrac, gfrac, tfrac	Fraction of coding nucleotides that are A, C, G or T
leadafrac, leadcfrac, leadgfrac, leadtfrac	Fraction of leading strand coding nucleotides that are A, C, G or T
lagafrac, lagcfrac, laggfrac, lagtfrac	Fraction of lagging strand coding nucleotides that are A, C, G or T
ggcfrac, cgcfrac	The G and C fraction of GC coding nucleotides respectively
atafrac, ttafrac	The A and T fraction of AT coding nucleotides respectively

Table 3. Fields in codongc.csv

123 The genomes.csv file contains the following fields:

fullname	The full chromosome name as found in the FASTA file
acount, ccount, gcount, tcount	Count of A, C, G or T nucleotides
plasmid	Set to 1 in case this sequence is a plasmid
realm1-5	NCBI sourced taxonomic data
protgenecount	Number of protein coding genes processed
stopTAG, TAA, TGA	Number of TAG, TAA and TGA stop codons respectively
stopXXX	Number of anomalous stop codons
startATG, GTG, TTG	Number of ATG, GTG and TTG start codons respectively
startXXX	Number of unusual start codons
dnaApos	position of DnaA gene (not DnaA box!) in the DNA sequence. -1 if not found.

Table 4. Fields in genomes.csv

124 Finally, the individual _fit.csv files contain fields called “Xskew” and “predXskew” to denote the observed X=gc, ta etc
125 skew, plus the prediction based on the parameters found in results.csv.

126 Technical Validation

127 This database models the skews of many chromosomes and plasmids. Validation consists of evaluating the goodness-of-fit
128 compared to the directly available numbers.

129 The *SkewDB* fits skews to a relatively simple model of only three parameters. This prevents overfitting, and this model has
130 proven to be robust in practice. Yet, when doing automated analysis of tens of thousands of chromosomes, mistakes will be
131 made. Also, not all organisms show coherent GC skew.

132 Figure 8 shows 16 equal sized quality categories, where it is visually clear that the 88% best fits are excellent. It is therefore
133 reasonable to filter the database on $RMS_{gc} < 0.1067$. Or conversely, it could be said that above this limit interesting anomalous
134 chromosomes can be found.

135 The DoriC database² contains precise details of the location of the origin of replication. 2267 sequences appear both in
136 DoriC and in the *SkewDB*. The DoriC origin of replication should roughly be matched by the “shift” metric in the *SkewDB*

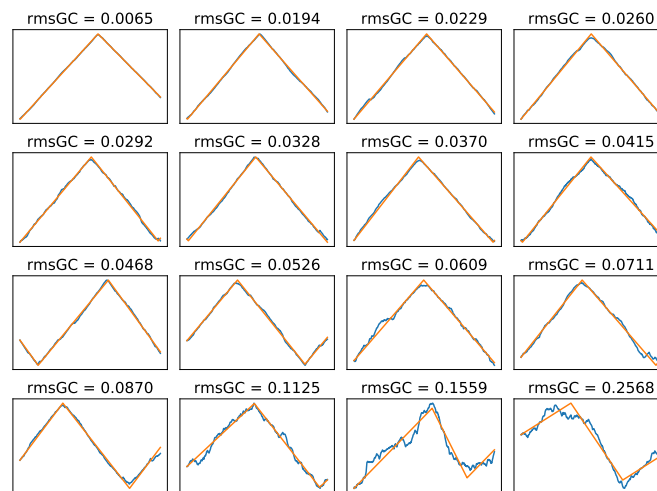


Figure 8. *SkewDB* fits for 16 equal sized quality categories of bacterial chromosomes

137 (but see Usage notes). For 90% of sequences appearing in both databases, there is less than 5% relative chromosome distance
138 between these two independent metrics. This is encouraging since these two numbers do not quite measure the same thing.

139 On a similar note, the *DnaA* gene is typically (but not necessarily) located near the origin of replication. For around 80% of
140 chromosomes, *DnaA* is found within 5% of the *SkewDB* “shift” metric. This too is an encouraging independent confirmation of
141 the accuracy of the data.

142 Finally, during processing numbers are kept of the start and stop codons encountered on all protein coding genes on all
143 chromosomes and plasmids. These numbers are interesting in themselves (because they correlate with GC content, for example),
144 but they also match published frequencies, and show limited numbers of non-canonical start codons, and around 0.005%
145 anomalous stop codons. This too confirms that the analyses are based on correct (annotation) assumptions.

146 Usage Notes

147 The existential limitation of any database like the *SkewDB* is that it does not represent the distribution of organisms found in
148 nature. The sequence and annotation databases are dominated by easily culturable microbes. And even within that selection,
149 specific (model) organisms are heavily oversampled because of their scientific, economic or medical relevance.

150 Because of this, care should be taken to interpret numbers in a way that takes such over- and undersampling into account.
151 This leaves enough room however for finding correlations. Some metrics are sampled so heavily that it would be a miracle if
152 the unculturable organisms were collectively conspiring to skew the statistics away from the average. In addition, the database
153 is a very suitable way to test or generate hypotheses, or to find anomalous organisms.

154 Finally it should be noted that the *SkewDB* tries to precisely measure the skew parameters, but it makes no effort to pin
155 down the Origin of replication exactly. For such uses, please refer to the *DoriC* database². In future work, the *SkewDB* will
156 attempt to use *OriC* motifs to improve fitting of this metric.

157 On <https://skewdb.org> an explanatory Jupyter¹¹ notebook can be found that uses *Matplotlib*¹² and *Pandas*¹³
158 to create all the graphs from this article, and many more. In addition, this notebook reproduces all numerical claims made in this
159 work. The *SkewDB* website also provides links to informal articles that further explain GC skew, and how it could be used for
160 research.

161 Code availability

162 The *SkewDB* is produced using the [Antonie DNA processing software](#), which is open source. In addition, once the RefSeq and
163 GenBank files have been created and from the NCBI website, the pipeline is fully automated and reproducible.

164 A [GitHub repository](#) is available for this article, which includes this reproducible pipeline, plus a script that regenerates all
165 the graphs and numerical claims from this paper.

166 References

167 1. Lu, J. & Salzberg, S. L. SkewIT: The Skew Index Test for large-scale GC Skew analysis of bacterial genomes. *PLOS*
168 *Comput. Biol.* **16**, e1008439, [10.1371/journal.pcbi.1008439](https://doi.org/10.1371/journal.pcbi.1008439) (2020).

- 169 2. Luo, H. & Gao, F. DoriC 10.0: an updated database of replication origins in prokaryotic genomes including chromosomes
170 and plasmids. *Nucleic Acids Res.* **47**, D74–D77, [10.1093/nar/gky1014](https://doi.org/10.1093/nar/gky1014) (2019).
- 171 3. O'Donnell, M., Langston, L. & Stillman, B. Principles and concepts of DNA replication in bacteria, archaea, and eukarya.
172 *Cold Spring Harb. Perspectives Biol.* **5**, a010108–a010108, [10.1101/cshperspect.a010108](https://doi.org/10.1101/cshperspect.a010108) (2013).
- 173 4. Lilly, J. & Camps, M. Mechanisms of theta plasmid replication. *Microbiol. Spectr.* **3**, [10.1128/microbiolspec.
174 plas-0029-2014](https://doi.org/10.1128/microbiolspec.plas-0029-2014) (2015).
- 175 5. Rudner, R., Karkas, J. D. & Chargaff, E. Separation of *B. subtilis* DNA into complementary strands. 3. Direct analysis.
176 *Proc. Natl. Acad. Sci.* **60**, 921–922, [10.1073/pnas.60.3.921](https://doi.org/10.1073/pnas.60.3.921) (1968).
- 177 6. Fariselli, P., Taccioli, C., Pagani, L. & Maritan, A. DNA sequence symmetries from randomness: the origin of the Chargaff's
178 second parity rule. *Briefings Bioinforma.* **bbaa041**, [10.1093/bib/bbaa041](https://doi.org/10.1093/bib/bbaa041) (2020).
- 179 7. Tillier, E. R. & Collins, R. A. The Contributions of Replication Orientation, Gene Direction, and Signal Sequences to
180 Base-Composition Asymmetries in Bacterial Genomes. *J. Mol. Evol.* **50**, 249–257, [10.1007/s002399910029](https://doi.org/10.1007/s002399910029) (2000).
- 181 8. Zhang, R. & Zhang, C.-T. A Brief Review: The Z-curve Theory and its Application in Genome Analysis. *Curr. genomics*
182 **15**, 78–94, [10.2174/1389202915999140328162433](https://doi.org/10.2174/1389202915999140328162433) (2014). Publisher: Bentham Science Publishers.
- 183 9. Charneski, C. A., Honti, F., Bryant, J. M., Hurst, L. D. & Feil, E. J. Atypical AT Skew in Firmicute Genomes Results from
184 Selection and Not from Mutation. *PLOS Genet.* **7**, e1002283, [10.1371/journal.pgen.1002283](https://doi.org/10.1371/journal.pgen.1002283) (2011).
- 185 10. Grigoriev, A. Analyzing genomes with cumulative skew diagrams. *Nucleic Acids Res.* **26**, 2286–2290, [10.1093/nar/26.10.
186 2286](https://doi.org/10.1093/nar/26.10.2286) (1998).
- 187 11. Kluyver, T. *et al.* Jupyter notebooks – a publishing format for reproducible computational workflows. In Loizides, F. &
188 Schmidt, B. (eds.) *Positioning and Power in Academic Publishing: Players, Agents and Agendas*, 87 – 90 (IOS Press,
189 2016).
- 190 12. Hunter, J. D. Matplotlib: A 2d graphics environment. *Comput. Sci. & Eng.* **9**, 90–95, [10.1109/MCSE.2007.55](https://doi.org/10.1109/MCSE.2007.55) (2007).
- 191 13. Reback, J. *et al.* pandas-dev/pandas: Pandas 1.3.2, [10.5281/zenodo.5203279](https://doi.org/10.5281/zenodo.5203279) (2021).
- 192 14. Hol, F. J. H., Hubert, B., Dekker, C. & Keymer, J. E. Density-dependent adaptive resistance allows swimming bacteria to
193 colonize an antibiotic gradient. *The ISME J.* **10**, 30–38, [10.1038/ismej.2015.107](https://doi.org/10.1038/ismej.2015.107) (2016).

194 Acknowledgements

195 I would like to thank Bertus Beaumont for helping me to think like a biologist, and Jason Piper for regularly pointing me to the
196 relevant literature. In addition, I am grateful that Felix Hol kindly allowed me to field test my software on his DNA sequences¹⁴.
197 Twitter users @halvorz and @Suddenly_a_goat also provided valuable feedback.

198 Author contributions statement

199 B.H. did all the work.

200 Competing interests

201 The author declares no competing interests.

202 Figures & Tables